Proceedings of ASME Turbo Expo 2011
GT2011
June 6-10, 2011, Vancouver, British Columbia, Canada

GT2011-45466

A THREE-DIMENSIONAL DIFFUSER DESIGN FOR THE RETROFIT OF A LOW PRESSURE TURBINE USING IN-HOUSE EXHAUST DESIGN SYSTEM

Sungho Yoon*, Felix Joe Stanislaus, Thomas Mokulys***, Gurnam Singh* and Martin Claridge***

* Alstom Power, Rugby, UK
** Infosys, Mysore, India
*** Alstom Power, Baden, Switzerland

ABSTRACT

The performance of the last stage of a Low Pressure (LP) steam turbine is strongly coupled with the downstream exhaust hood performance. In particular, the effect of the diffuser within the exhaust hood on the pressure recovery is very important in retrofitting existing machines, which dictate many geometric constraints.

Alstom's in-house Exhaust Design System (EDS) simulates the three-dimensional flow in the exhaust hood by coupling the last stage blades and the exhaust hood. This EDS system can be used to design an LP diffuser in the exhaust hood and to achieve the required performance targets. In the first part of this paper, the EDS system is validated against measurements within model turbines, which represent both a standard machine as well as a retrofit machine.

In the second part of this paper, an LP diffuser was re-designed to improve the performance using the EDS method. To begin with, an axi-symmetric diffuser was designed using numerical simulations of a passage in the last stage turbine as well as a slice of the diffuser and the exhaust hood. By carefully controlling the profile of the diffuser casing, the flow separation at the original casing walls was reduced significantly and this, in turn, improved the performance of the turbine substantially. Then, the full geometry of the exhaust hood was modeled in order to investigate the effect of the three-dimensional flow features. Based on the examined flow features, an asymmetric change was introduced to the diffuser casing to improve the three-dimensional flow structure. This new asymmetric diffuser was found to maximize the exhaust performance.

NOMENCLATURE

a	Speed of sound
c_p	Specific heat capacity at a constant pressure
h	Enthalpy
KE	Kinetic Energy
l	Axial length between the last stage blade to the exhaust wall
M	Mach number
$\dot{m}$	Mass flow rate
PR	Pressure ratio
p	Pressure
s	span
T_q	Torque
V	Velocity
ω	Rotational speed
η	Efficiency
γ	Specific heat ratio
χ	Pressure recovery coefficient

Subscripts

0,1	stage inlet, stage exit (diffuser/exhaust inlet),
2,3	diffuser exit, exhaust exit
tot	total
z	axial direction
is	isentropic
ave	averaged

INTRODUCTION

Meeting the rising energy demand and mitigating its environmental impact is a main challenge in modern society. In order to address this issue, Alstom has advanced various technologies from renewable energy to the retrofit of existing power plants. In particular, Alstom has successfully retrofitted and upgraded many steam turbines in the past decades to increase the power output from existing power plants. An example can be found in Haller and Hesketh [1]. It has been found that the design of the Low Pressure (LP) diffuser is particularly challenging in a retrofit project because the original exhaust geometry often limits the design scope. Therefore, it is the aim of this paper to demonstrate the challenges of designing LP diffusers in the exhaust hood and share some lessons learned.

Power output from the LP turbine can be maximized by minimizing the pressure downstream of the last stage blade row, for given turbine blades and a fixed exhaust outlet pressure [Tindell et al., 2]. This can be achieved by increasing the pressure recovery in the exhaust hood. In order to improve the pressure recovery in the exhaust hood, it is essential to understand the flow physics within the exhaust hood.

Significant progress has been made in understanding the flow structures and its associated loss mechanism in a turbomachinery blade as demonstrated by Denton [3]. However, the understanding of the flow physics in the exhaust hood is not yet mature and it is still quite challenging to quantify the loss mechanisms in the exhaust hood. Flows in the exhaust hood experience various loss mechanisms. Firstly, the flow leaving the last stage of the LP turbine generally enters an axial-radial diffuser where the flow is turned 90° in a short distance (A in Fig. 1). Although a lot of understanding has been gained and many quantitative correlations were derived in a conventional axial diffuser [Sovran and Klomp, 4], they cannot be directly applied to the axial-radial diffuser encountered in the LP steam turbine exhaust. The pressure recovery in the axial-radial diffuser is determined by various parameters, which include the area ratio, aspect ratio (l/s), the diffuser casing profile and the diffuser hub profile. Secondly, at the downstream side of the diffuser exit in the upper hood, the fluid is turned 180° and flows downward towards the exhaust exit (B1 in Fig. 1). It should also be noted that a fraction of the fluid in the upper hood passes over the diffuser casing, towards the center of the exhaust hood, and moves towards the exhaust exit (B2 in Fig. 1). Thirdly, flow from the upper diffuser will mix out with flows from the lower diffuser (C in Fig. 1). This mixing loss is often accompanied by loss due to mechanical struts which stiffen the exhaust hood.

Moreover, the performance in the exhaust hood is strongly coupled with the performance of the last stage of the LP turbine including the tip leakage flow. There have been several studies to understand the interaction between last stage blade rows and the exhaust hood. Liu et al. [5] showed that the inlet condition upstream of the LP diffuser affects the flow in the diffuser and the exhaust hood significantly. Kreitmeier and Greim [6] also demonstrated the interaction between the last stage blade and the exhaust hood affects the performance of the exhaust substantially. Recently, Fu and Liu [7] demonstrated that different radial distribution of swirl angles, upstream of the LP diffuser, affects the pressure recovery in the exhaust hood.

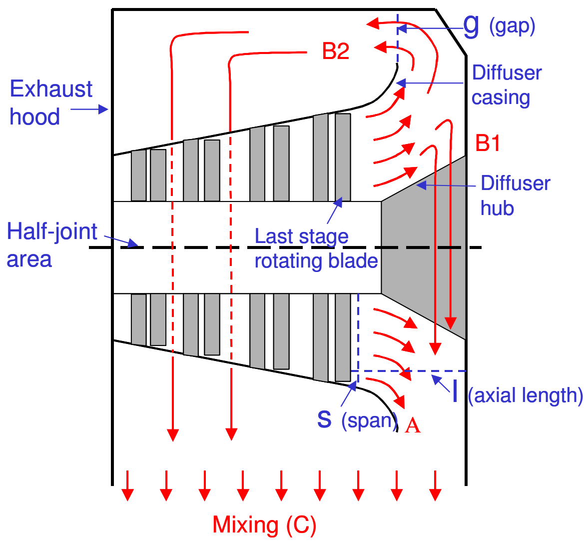

Fig. 1 Flow features in the exhaust hood

Because of the complexity of the flows, the studies of the exhaust hoods were mainly based on experimental tests in the past [Cofer, 8]. When a prediction is required, it has traditionally been assumed that the kinetic energy downstream of the last stage blade is dissipated. Alternatively, several correlations have been developed based on measurements on model exhaust hoods such as Craig and Cox [9], Spencer et al. [10] and Cotton [11].

Over the last few decades, due to the increase in available computer power, there has been a significant advances in three-dimensional (3D) numerical methods. Solving the 3D Navier-Stokes or Euler equations enables turbine designers to better understand 3D flow features. Consequently, the use of these 3D numerical methods has become a design routine for the turbine industry as shown by McBean et al.[12]. Although it is more common to use 3D simulations for a single turbine blade passage, these numerical methods are slowly being used to model more complex systems such as the exhaust hood. Furthermore, some optimization studies for exhaust systems were recently conducted based on the 3D numerical methods as demonstrated by Hongtao et al. [13]. However, the biggest challenge in simulating an exhaust hood is to model the interaction effect with the last stage LP turbine blade row, capturing the radial and circumferential variation of flow characteristics. In particular, the asymmetry of the exhaust hood causes a significant variation of the circumferential flow field downstream of the last stage blade. Ideally, modeling the full annulus including the last stage blades and the exhaust hood would correctly represent this circumferential variation of the flow field. However, this will incur enormous computational power and, therefore, is seldom attempted[1]. Moreover, industrial design generally necessitates an overnight simulation, requiring a more practical approach by modeling the interaction between the last stage blades and the exhaust hood.

In order to account for the effect of the last stage turbine blade rows on the exhaust hood, Liu and Hynes [14, 15] applied a numerical actuator disc where flow properties jump to achieve required flow turning and entropy rise across the blade row. By using this numerical disc, the circumferential flow field at the diffuser inlet was modeled and a realistic 3D numerical simulation on the exhaust hood was conducted. The advantages of using this actuator disc are its simplicity and fast computational speed. However, the actuator disc is not able to predict the tip leakage flow accurately and this will change the flow behavior at the diffuser casing significantly. Moreover, the actuator disc cannot predict choking behavior since it does not have the detailed geometric information of the turbine blade. In order to overcome these problems, Alstom developed an in-house procedure called Exhaust Design System (EDS). This EDS procedure couples the last stage blades and the exhaust hood, as recently presented by Beevers et al. [16]. By using the EDS method, the detailed flow behavior such as radial and circumferential distribution downstream of the last stage blade row can be captured correctly and fed into the analysis of the exhaust hood. In addition, choking behavior as well as the tip leakage flow can be correctly predicted. This EDS method will be explained further and validated against measurements in this paper.

The design of the LP diffuser is crucial in increasing the pressure recovery in the exhaust hood. Compared to the generally unguided flows in the exhaust hood, flows in the diffuser can be well controlled and a substantial pressure recovery can be achieved. Traditionally, LP diffusers were designed to be axi-symmetric. Moreover, the design of LP diffusers were often based on numerical simulations on a single blade passage of the LP turbine without taking into account the detailed geometric details of the exhaust hood. However, the LP diffuser needs to be designed by considering the exhaust hood. This is particularly true in a retrofit project because a relatively smaller exhaust hood, compared to the new equipments, often affect the diffuser performance. It will be demonstrated that a good performing diffuser in a large exhaust hood may not perform well when a relatively small exhaust hood is utilized. This requires a 3D (or asymmetric) diffuser design as will be discussed in this paper.

[1] Beevers et al. [16] estimated that above 25 million grid nodes are required for the full annulus simulations.

OUTLINE OF THE PAPER

The outline of this paper consists of two main parts. In the first part, numerical predictions based on the EDS calculations are validated against measurements. Experimental work was conducted on two exhaust hoods that represent a standard exhaust hood and a retrofit exhaust hood where a diffuser was implemented in the existing exhaust hood. Both exhaust hoods have the same LP last stage blades. In addition to the comparison between the predictions and measurements, challenges in the retrofit project will be demonstrated.

In the second half of this paper, an LP diffuser casing is optimized based on numerical simulations using the EDS calculations. This optimization procedure consists of the following two procedures. Firstly, the re-design of the diffuser casing profile is conducted based on a stage calculation, assuming an axi-symmetric diffuser. Secondly, the optimization considers the full annulus and the surrounding exhaust hood. It will be demonstrated that a circumferential variation of the diffuser casing can maximize the pressure recovery in the exhaust hood. Finally, conclusions are drawn based on the results.

PART I: EDS AND ITS EXPERIMENTAL VALIDATION

EXHAUST DESIGN SYSTEM (EDS)

EDS is an in-house procedure that couples the last stage blades of the LP turbine and the exhaust hood downstream of the last stage blades and it was previously described in Benim et al. [17] and Beevers et al. [16]. This routine is able to simulate correct circumferential and radial variation of the flow downstream of the last stage blades, while reducing the computation time significantly. Different in-house and commercial solvers can be used with the EDS calculations because the coupling process is code independent. In this study, a commercial program, CFX, is employed as a flow solver.

The EDS method consists of two consecutive procedures. Firstly, stage calculations are performed and these calculations include a stationary blade, a rotating blade and a slice of the diffuser and the exhaust hood that correspond to the single rotor passage. By conducting stage calculations over a range of operating conditions, a database is established which relates the two planes: one is placed at the trailing edge of the last stage blade and the other is located further downstream, as will be shown in Fig. 7. This database is fed to the second procedure.

As a second step, the full exhaust hood downstream of the last stage blades is modeled. For a fixed exhaust exit boundary condition, the inlet boundary condition to the exhaust hood is determined based on the database by calculating the solution in an iterative manner. To begin with, a circumferentially uniform inlet boundary condition is applied. After the first calculation, the inlet boundary condition is updated based on the flow characteristics at the coupling plane. In order to capture the circumferential variation at the exhaust inlet (downstream of the blade trailing edge), the exhaust inlet boundary plane as well as the coupling plane is segmented into over a hundred smaller circumferential pieces and each segment's flow properties are updated after each iteration. By iterating this procedure several times, a realistic asymmetric inlet boundary condition can be produced.

The current EDS assumes a perfect gas with steam representative flow properties of the specific heat capacity at a constant pressure (c_p) and the specific heat ratio (γ). The EDS calculations do not account for the wakes from the blades, unsteady flow effects and wetness effects. Further details of the EDS method can be found in Beevers et al. [16].

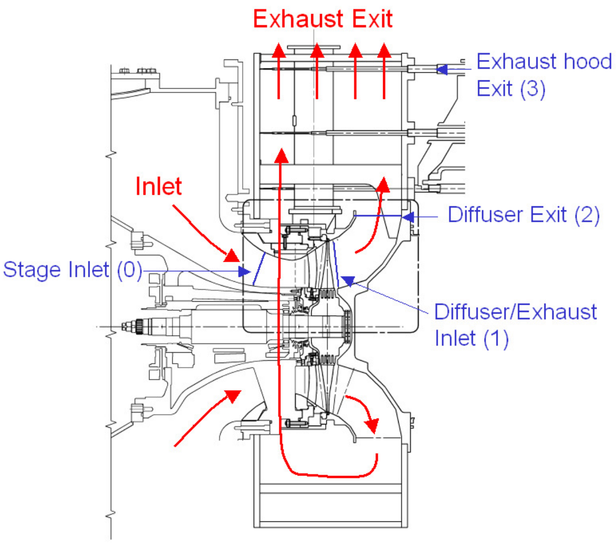

Fig. 2 Model turbine facility

EXPERIMENTAL METHOD

An experimental turbine rig, which is an approximately 10% scale of a real turbine, is used for the measurements and is shown in Fig. 2. The model turbine was tested over a range of pressure ratios (the inlet plenum total pressure to the exhaust exit static pressure, PR=$p_{tot,0}/p_3$) ranging from 3.0 to 5.2. In order to achieve a desired pressure ratio, the downstream pressure (p_3) is varied by changing the exhaust exit pressure, while the upstream total pressure ($p_{tot,0}$) is fixed due to constant inlet flow conditions. The working fluid in the rig is a mixture of 93% R134a and 7% air by weight. By utilizing a mixture of fluids and running the model turbine at a high rotational speed, a real machine representative Mach number and loading coefficient is achieved. Although the Reynolds number in the model turbine is 73% of that in the real machine, CFD studies showed that the effect of Reynolds number is negligible in this flow regime.

Static pressure tappings are installed at the inlet and exit of the stationary blade, the inlet and exit of the rotating blade, the diffuser hub and casing and the walls of the exhaust hood. Moreover, several traverse planes are installed at the stage inlet, stage exit (diffuser inlet), diffuser exit, exhaust hood exit. Overall total to static efficiency of the turbine is calculated by:

$$\eta = \frac{T_q \times \omega}{\dot{m} \times \Delta h_{is}} \tag{1}$$

Δh_{is} represents the isentropic enthalpy drop from the inlet total to exhaust static condition. Shaft power is measured via a load cell on the dynamometer. The repeatability of the efficiency measurement is within ±0.1%. Another important parameter is the pressure recovery coefficient of the exhaust hood and this parameter can be defined as the isentropic enthalpy increase (Δh_{is}) in the exhaust hood relative to the leaving kinetic energy (KE_1) at the inlet of the exhaust hood:

$$\chi = \frac{\Delta h_{is}}{KE_1} = \frac{\frac{a^2}{(\gamma-1)}\left[\left(\frac{p_3}{p_1}\right)^{\frac{\gamma-1}{\gamma}} - 1\right]}{\frac{1}{2}V_1^2} = \frac{2}{(\gamma-1)M_1^2}\left[\left(\frac{p_3}{p_1}\right)^{\frac{\gamma-1}{\gamma}} - 1\right] \tag{2}$$

Equation (2) shows that the pressure recovery coefficient is mainly dependent on the Mach number at the exhaust inlet (M_1), pressure at the exhaust inlet (p_1) and the exhaust exit (p_3). In order to calculate the pressure at the exhaust inlet, both static pressure measurements at the endwalls and radial traverse measurements through the span were utilized. Six static pressures were measured on the casing and on the hub, respectively, and they are arithmetically averaged to represent the averaged pressure on both the casing and the hub. Three circumferentially different traverses were conducted at the diffuser inlet with approximately 120° circumferential space. These three traverses are also arithmetically averaged to represent the radial pressure gradient at the diffuser inlet. It should be noted that it is ideal to have more circumferentially different traverse positions. However, considering the three traverse positions are equally spaced, the averaged value is considered to be representative of the true average pressure.

Figure 3 shows radial pressure distributions at different pressure ratios. It was found that the averaged traverse pressure agrees well with the averaged static pressures near the casing and the hub. It is also worth noting that the pressure drops sharply near the casing because the flow accelerates near the diffuser casing due to the convex curvature of the diffuser casing. Pressure at the diffuser inlet (p_1) can be calculated for each pressure ratio by conducting area-averaging using both the traverse data as well as the static pressure measurements on the endwalls. At the exhaust exit, traverse measurements showed that the static pressure was uniform. Therefore it was sufficient to use the measured twelve static pressures on the hood in order to estimate the characteristic mean pressure at the exhaust exit (p_3).

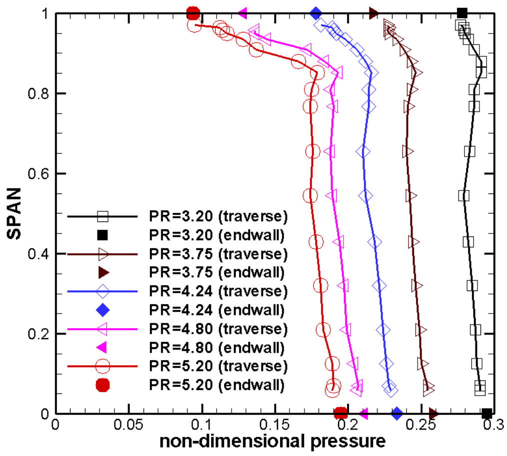

Fig. 3 Radial distribution of the non-dimensional static pressure ($p_1/p_{tot,0.ave}$) at the exhaust inlet for the standard exhaust hood

EXPERIMENTAL AND NUMERICAL RESULTS

In order to validate the EDS method and demonstrate challenges in a retrofit design, experimental studies were conducted for two different exhaust hoods of the model turbine, with the same last stage blades. One is a standard exhaust hood and the other is a retrofit exhaust hood. A vertical section of the two different exhaust hoods are compared in Fig. 4. It can be seen that the exhaust hood for the retrofit has a smaller aspect ratio and smaller gap between the inner cylinder and the exhaust compared to that of the standard exhaust hood. It can be also found that the retrofit exhaust hood experiences much higher pressure, particularly near the hub, which effectively reduces the pressure recovery in the exhaust hood and the turbine power output for a fixed exhaust hood exit condition.

Figure 5 shows the measured pressure recovery coefficients of the two exhaust hoods. The retrofit exhaust hood resulted in a poorer performance than the standard exhaust hood. When the pressure ratio is 5.2, the decrease in the pressure recovery coefficient is about 0.6, which corresponds to 60% of the kinetic energy at the stage exit. This reduction in the recovery coefficient would decrease the turbine power output and efficiency by increasing the pressure downstream of the last stage blades. When the pressure ratio is 5.2, the retrofit machine was found to reduce the power output of the single stage turbine stage by 11% compared to the standard machine.

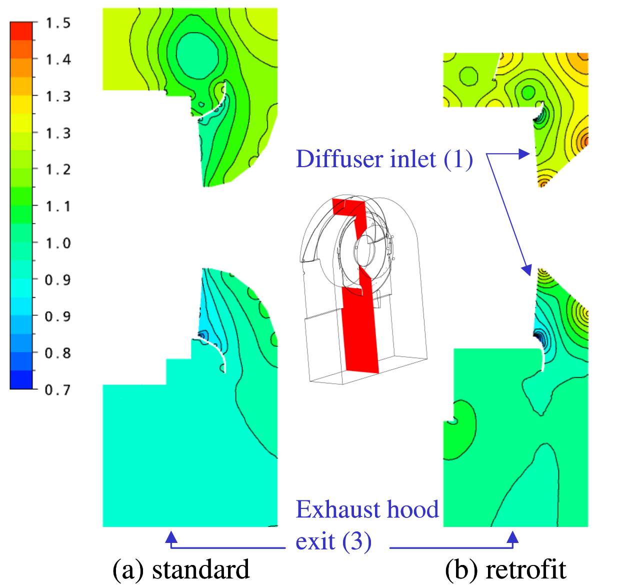

Fig. 4 Normalised pressure ($p/p_{3.ave}$) contours in the standard and retrofit exhaust hoods for the same exhaust exit condition

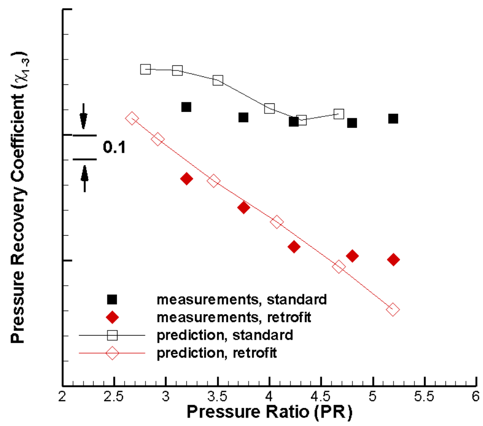

Fig. 5 Comparison of the pressure recovery of the two exhaust hoods against the pressure ratio ($PR=p_{tot,0}/p_3$)

Predicted results, based on the EDS calculations, are also compared in Fig. 5. The numerical scheme and grid resolution are not described in detail because they are similar to those of the EDS calculations described in the second part of this paper. It can be seen that predicted the pressure recovery coefficient reasonably well. More importantly, the EDS calculations predicted correctly the change in the pressure recovery when the two different exhaust hoods are compared. This shows the validity of the method as a design tool.

It is important to note that a change in the exhaust hood can reduce the performance significantly although they use the same last stage blades. A challenge in retrofitting existing machines is to design an LP diffuser taking into account a relatively small exhaust hood. A design strategy of the LP diffuser in a retrofit machine will be demonstrated in the second part of this paper.

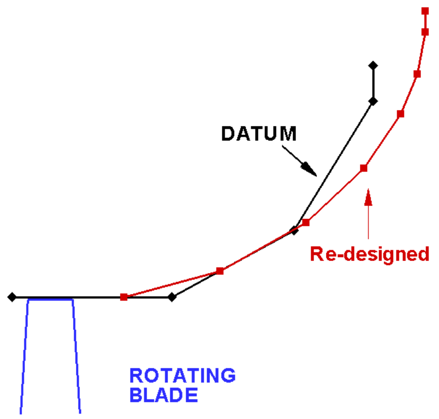

Fig. 6 Profile of the diffuser casing in the meridional plane

PART II: RE-DESIGN OF AN LP DIFFUSER USING EDS

DATUM TURBINE

The datum turbine for the second part of this paper is based on a nuclear power plant. The power plant has three double-flow LP cylinders and the original machine was manufactured by a different steam turbine company. The machine runs at 1800 rpm and originally produced approximately 1,000 MW. Recently, Alstom retrofitted the LP module including longer last stage blades. The recent site measurements confirmed that a guaranteed performance was achieved, increasing the turbine power output by 35 MW[2] relative to the original machine.

The aim of this study is to optimize the LP diffuser downstream of the last stage blades and to maximize the turbine power output. The optimization procedure using the EDS method follows two steps. Firstly, an axi-symmetric diffuser is assumed and the optimum profile of the diffuser casing in the meridional plane is chosen based on a single blade passage calculations. Secondly, the full 3D diffuser casing is optimized considering the detailed exhaust hood geometry. In order to begin the design process, a datum diffuser[3] casing, shown in Fig. 6, was selected with three kinks which change the flare angle from 0° to 90° in 30° increments.

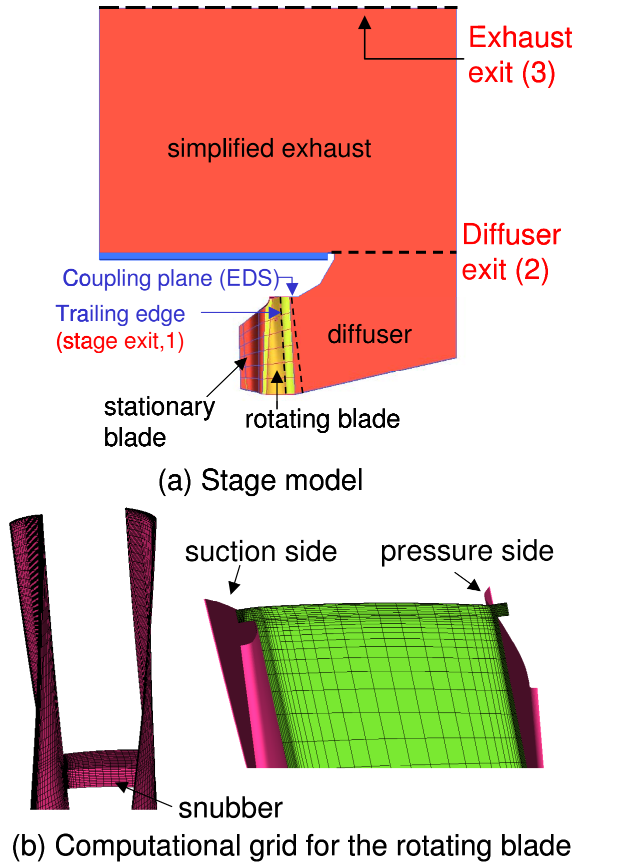

Fig. 7 Computational model for the last stage blades and diffuser calculation

AXI-SYMMETRIC DIFFUSER DESIGN

As a first step of the design process, a stage calculation was conducted, simulating a passage of the stationary blade and the rotating blade and a slice of the diffuser and the exhaust hood as shown in Fig. 7. In order to model the diffuser part, an axi-symmetric diffuser was assumed. In addition, a very simplified

[2] This improvement is mainly due to the use of aerodynamically efficient blades and the diffuser.

[3] This datum diffuser is a starting geometry for the design study. The datum geometry was selected because similar geometries are found in the existing machines.

large exhaust hood is modeled without considering the detailed 3D geometry. A more accurate modelling of the diffuser and the exhaust will be considered in the second step of the EDS design process, which will be described in the next section.

A commercial grid generation program, ICEM-CFD 11, was employed to model the turbine stage. Another commercial numerical program, CFX 11, is used as a flow solver. Both the tip clearance above the rotor tip and the snubber were modeled in the rotating blade. Hexahedral mesh was used in order to represent the geometry. A mixing plane was used between the stationary blade and the rotating blade. About a million nodes were used to model the geometry. Second Order (High Resolution) discretization was utilized and a standard k-epsilon model was employed for a turbulence model. In order to speed up the calculation, a scalable wall function was used. Calculated y^+ on the walls ranged from 20 to 60.

To begin with, a stage calculation was conducted at the design pressure ratio for the datum geometry shown in Figs. 6 and 7. It was found that the datum diffuser resulted in a significant separation on the diffuser casing from the first kink where the flare angle changes sharply from 0° to 30° as shown in Fig. 8(a). This separation is detrimental to the performance because it causes not only aerodynamic losses but also a reduction in the effective flow area at the radial exit of the diffuser. The effective flow area at the diffuser exit is about 30% less than the geometric area of the diffuser exit. Consequently the pressure recovery in the diffuser is low due to both aerodynamic loss and reduced effective area at the diffuser exit. Fig. 8(b) shows that there is no significant pressure recovery near the diffuser casing, although some pressure recovery is achieved near the diffuser hub. Overall, this resulted in a poor pressure recovery, which in turn caused a relatively high pressure downstream of the last stage blade. This is particularly evident near the casing in Fig. 8(b).

In order to minimize the flow separation and improve the pressure recovery, a new diffuser casing was designed by carefully controlling the diffuser casing flare angle with multiple kinks as shown in Figure 6(b). Figure 9 shows the pitchwise mass-averaged meridional Mach number and pitchwise area-averaged pressure in the meridional plane. Meridional Mach number contour shown in Fig 9(a) shows that the re-designed diffuser helps the flow to remain attached to the outer casing of the diffuser, whereas the datum diffuser resulted in a significant separation. Therefore the geometric area at the diffuser exit is fully utilised to recover the pressure. Fig 9(b) also shows that a good pressure recovery is achieved throughout the diffuser. In particular, the pressure recovery near the diffuser casing is significantly improved compared to the datum shown in Fig. 8(b).

For a given exhaust exit pressure (fixed pressure ratio, $p_{tot,0}/p_3$), a good pressure recovery reduces the pressure and increase the Mach number at the exit of the last stage blade with the consequence of increasing the expansion through the turbine stage and the power output. The higher Mach number at the exit of the rotating blade and a further expansion near the diffuser casing, due to its curvature, caused a strong shock near the diffuser casing. Another shock is also predicted downstream of the rotating blade from the hub to the mid-span. Although these shocks lead to entropy generation and reduce the total pressure, the overall pressure recovery coefficient based on Eq. (2) increased by 0.4 relative to the datum. This can be understood that 40% more kinetic energy was recovered by re-designing the diffuser casing.

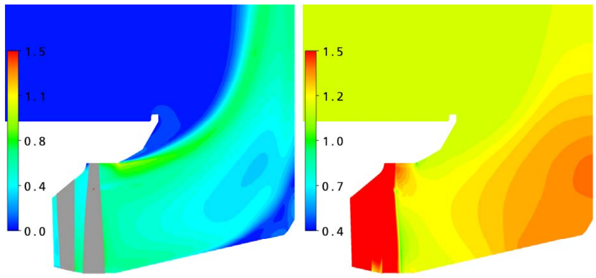

(a)Meridional Mach number (b) Non-dimensional pressure ($p/p_{3.ave}$)

Fig. 8 Pitchwise-averaged flow field with the datum diffuser in the meridional plane at the design pressure ratio

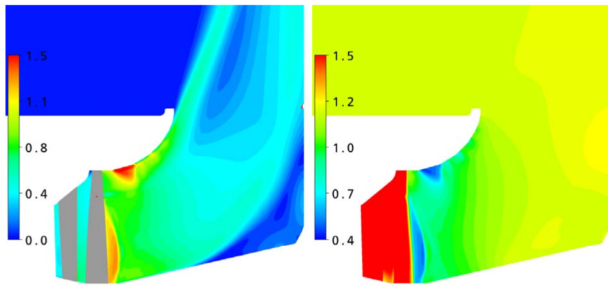

(a)Meridional Mach number (b) Non-dimensional pressure ($p/p_{3.ave}$)

Fig. 9 Pitchwise-averaged flow field with the re-designed diffuser in the meridional plane at the design pressure ratio

Finally, the performance was predicted over a range of operating conditions and the performance of the two axi-symmetric diffusers is compared in Figure 10. It is important to predict the performance at various operating conditions for two reasons. Firstly, a power plant operates throughout a year with various condenser pressures. Therefore it is necessary that the re-designed diffuser achieves a good performance throughout the year. Secondly, in a real 3D exhaust hood, the diffuser exit effectively experiences different back pressures around the circumference due to the asymmetry of the exhaust hood even for a fixed exhaust hood exit condition. This necessitates producing a database corresponding to different operating conditions from the stage calculations. This database enables the numerical prediction of a three-dimensional exhaust hood, using the EDS calculations, to be possible.

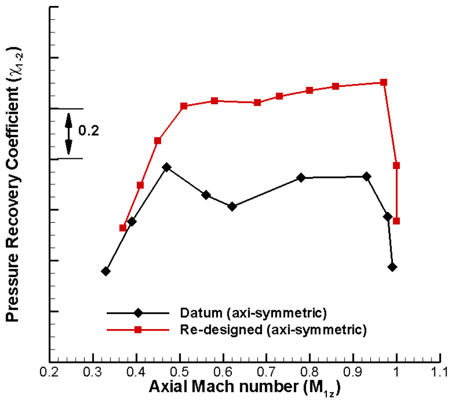

Fig. 10 Performance comparison of the datum and the re-designed (axi-symmetrically re-profiled) diffuser

It can be clearly seen from Fig. 10 that the re-designed (axi-symmetrically re-profiled) diffuser increases the performance substantially over a range of operating conditions. It is also worth noting that the pressure recovery coefficient drops significantly when the axial Mach number approaches the sonic speed. As the axial Mach number approaches the sonic speed, the flow information cannot propagate upstream and the power from the last stage turbine cannot be enhanced further; the turbine blade experiences "limit load" with the production of the maximum power output.

Traditional diffuser design often finishes here and axi-symmetric diffuser casing is manufactured. However, it is the authors' experience that the LP diffuser should be further optimized considering the detailed exhaust hood geometry. This is particularly important in a retrofit because a small exhaust hood blocks the flow in various parts of the exhaust hood and reduces the diffuser performance. Therefore, a further 3D optimization of the diffuser casing, considering the full geometry of the exhaust hood, was conducted and will be described in the next section.

THREE-DIMENSIONAL DIFFUSER DESIGN

The detailed geometric features of the exhaust hood including the LP diffuser was modelled to conduct the EDS calculations and investigate 3D flow features in the exhaust hood. The actual exhaust geometry was modelled including various splitters and mechanical struts as shown in Fig. 11(a). Fig. 11(b) shows the datum diffuser casing relative to the exhaust hood. It is important to note that the radial gap between the diffuser casing and surrounding exhaust hood is small as shown in Fig. 11(b). In order to fit the exhaust hood, the upper section of the diffuser casing had to be trimmed. Moreover, additional parts below the half-joint area were also trimmed to accommodate mechanical struts which sustain the exhaust hood.

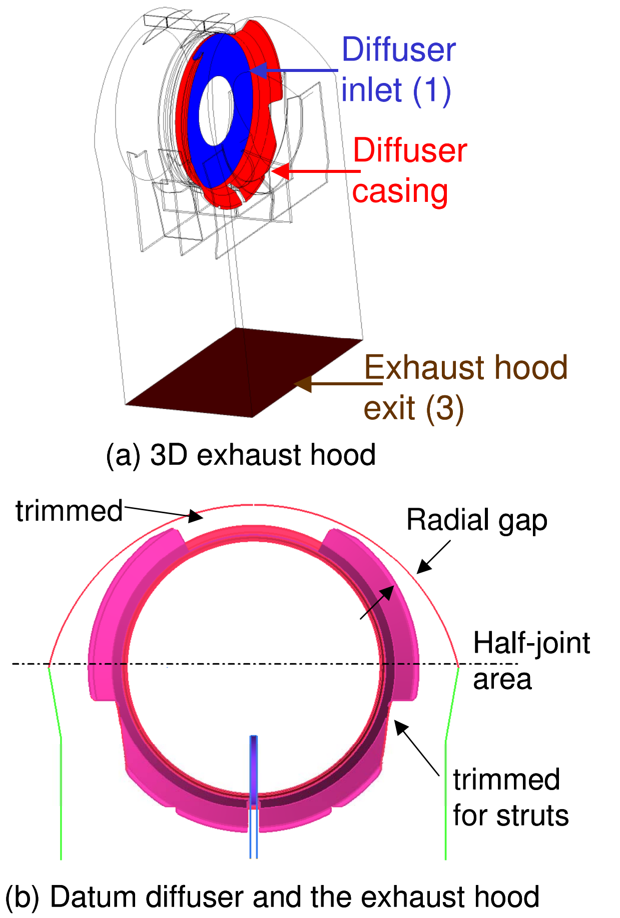

Fig. 11 Exhaust hood model for the EDS calculations

The small radial gap between the diffuser casing and the exhaust hood tends to prevent the flow passing over the diffuser casing in the upper hood. (Flow B2 in Fig. 1). This feature effectively reduces the flow area in the downstream and causes more mixing loss, resulting in a reduced pressure recovery in the exhaust hood. Since the re-designed diffuser casing shown in Fig. 6 has a larger diameter, the gap between the diffuser casing and the exhaust hood is smaller and, consequently, the penalty due to this small gap would be even more severe.

Due to the complexity of the model, tetrahedral mesh was employed to generate the grid for the geometry. The number of elements and nodes for the model is approximately 5 million and 1.6 million, respectively. This resulted in y^+ between 15 and 80. A similar numerical scheme to that used in the stage calculations was applied in the EDS calculations. The inlet boundary conditions for the exhaust hood are determined by the database generated in stage calculations by an iterative procedure.

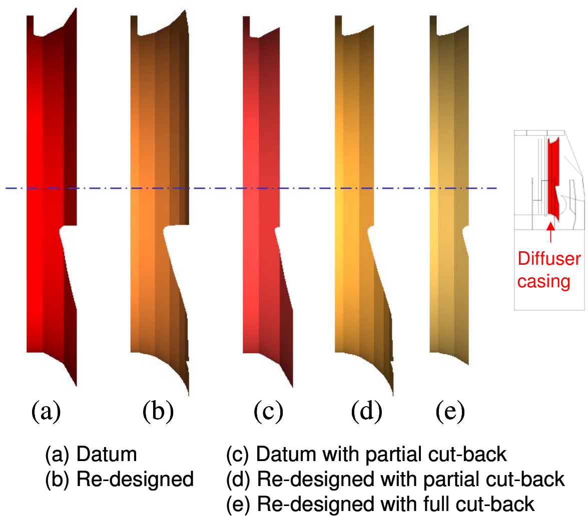

Fig. 12 Side view of the examined geometries for diffuser casing

Geometries	$\Delta\chi_{1-3}$
Datum	-
Re-designed	-0.27
Datum with a partial cut-back	0.17
Re-designed with a partial cut-back	0.38
Re-designed with a full cut-back	-0.05

Table 1 Improvement of the pressure recovery coefficient relative to the datum at the design operating condition

Five different diffuser geometries were examined as shown in Fig 12. The first two geometries correspond to the datum and the re-designed diffuser casing, which are based on Fig. 6 and were described in the previous section. The only difference from the previous section is that a realistic 3D diffuser casing is modeled as shown in Fig. 11(b). The third and the fourth geometries introduce a partial cut-back in the upper hood. This cut-back was introduced to increase the radial gap between the diffuser casing and the exhaust, considering the small radial gap is detrimental for the performance of the exhaust hood. These two geometries with a partial cut-back have the same radial gap size between the diffuser casing and the exhaust hood. The fifth geometry introduces a full cut-back around the full circumference. This was examined to investigate further the effect of a cut-back on the exhaust hood performance. The predicted improvement of the pressure recovery coefficient (χ_{1-3}), from the diffuser inlet (1) to the exhaust exit (3) at the design operating condition, is summarised in Table 1.

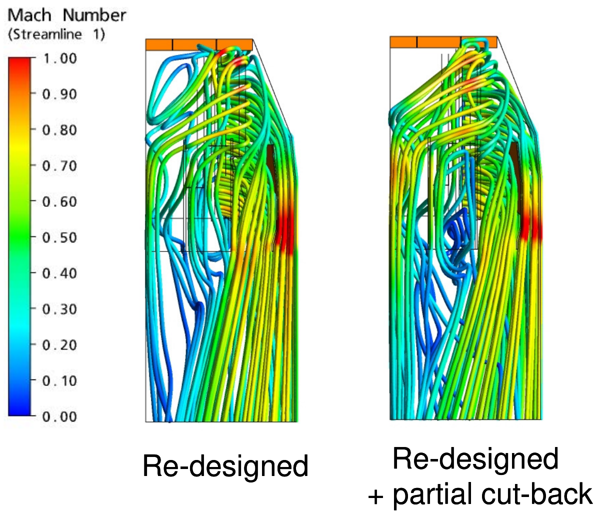

Fig. 13 Streamlines in the exhaust box

Firstly, the redesigned diffuser casing was compared with the datum. The re-designed diffuser casing decreased the pressure recovery coefficient in the exhaust hood by 0.27 relative to the datum. Although the re-designed diffuser eliminates the flow separation and performs better than the datum as a diffuser, the reduced gap between the diffuser casing and the exhaust hood reduced the performance significantly. Fig. 13 shows the streamlines in the exhaust hood. When the re-designed diffuser casing is used, only a small amount of fluids flow over the diffuser casing in the upper hood. Fig. 14 shows the normalized total pressure at the half-joint area. The re-designed diffuser casing increased the non-uniformity of the total pressure, which would cause more mixing loss downstream and increase the kinetic energy at the exit of the exhaust hood. It is also worth noting that the flow field is not symmetric in Fig. 14 because the flow downstream of the last stage blade is not purely meridional but has some tangential velocity components.

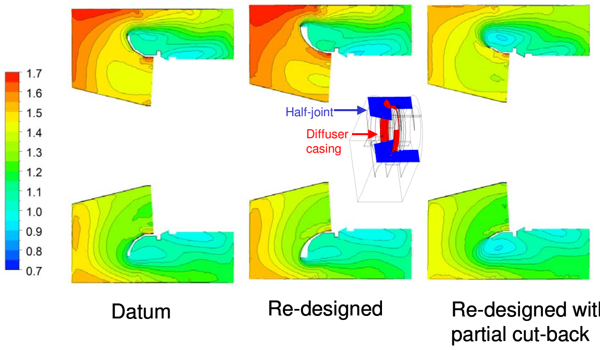

Fig. 14 Normalized total pressure ($p_{tot}/p_{3.ave}$) contour at the half-joint area

In order to overcome the blockage effect due to the small gap, a partial cut-back that covers the upper hood, as shown in Fig. 12, was introduced to both the datum and the re-designed diffuser, resulting in an asymmetric diffuser casing. This asymmetric diffuser casing increased the radial gap and enhanced the performance in both the datum and the re-designed diffuser relative to the datum as summarised in Table 1. A better performance was achieved with the re-designed diffuser casing because the re-designed diffuser casing results in a good pressure recovery without flow separations, whereas the datum diffuser casing causes some flow separations with a poor pressure recovery. This means that the optimization procedure in the previous section (Axi-symmetric diffuser design), assuming an axi-symmetric diffuser casing, is still a necessary procedure before the final 3D optimization. The increased recovery coefficient is 0.38 relative to the datum, which corresponds to 38% of the leaving kinetic energy.

Fig. 13 shows that the introduction of a partial cut-back increases the flow over the diffuser casing in the upper hood. Moreover, Fig 14 also shows that the total pressure became more uniform at the half-joint area. In particular, the very high total pressure on the back wall (left wall in Fig. 13) was reduced significantly, which will reduce the skin friction loss on the wall as well as the mixing loss downstream. Moreover, the more uniform flow will effectively reduce the kinetic energy at the exit of the exhaust hood, resulting in a higher pressure recovery.

A full cut-back, which covers the full circumference, was introduced in order to examine whether a further cut-back helps to increase the pressure recovery. The numerical simulation indicates that this further cut-back decreases the pressure recovery relative to the datum as well as the re-designed diffuser casing with a partial cut-back. The re-designed diffuser casing in the lower hood was contributing to the pressure recovery without flow separation. Consequently, a further cut-back in the lower hood does not improve but decreases the pressure recovery in the exhaust hood.

Finally, the performance of the datum and the optimized (re-designed with a partial cut-back) diffuser casing, using the same last stage of the LP turbine, was examined over seven different pressure ratios using the EDS calculations. Fig. 15 shows the pressure recovery coefficient ($\chi_{1\text{-}3}$) and the total to static efficiency ($\eta_{0\text{-}3}$) defined from the inlet of the last stage (0) to the exhaust exit (3) against the axial Mach number (M_{1z}) at the diffuser inlet. It should be noted that the $\chi_{1\text{-}3}$ in Fig. 15 accounts for the detailed three-dimensional geometric features of the exhaust hood, whereas $\chi_{1\text{-}2}$ in Fig. 10 does not. Due to the various loss mechanisms in the exhaust hood, explained in the beginning of this paper, the characteristics of $\chi_{1\text{-}3}$ in Fig. 15 is different from $\chi_{1\text{-}2}$ in Fig. 10.

Fig. 15 clearly shows that the optimized diffuser casing improved both the pressure recovery and the efficiency significantly throughout operating conditions. It should be pointed out that the performance decreases sharply when the axial Mach number is greater than 0.8. This is due to the fact that some parts of the last stage blade, particularly in the lower hood, starts to experience limit load with the axial Mach number reaching 1. The results discussed in this section demonstrate the importance of considering the full 3D exhaust hood and designing the diffuser accordingly.

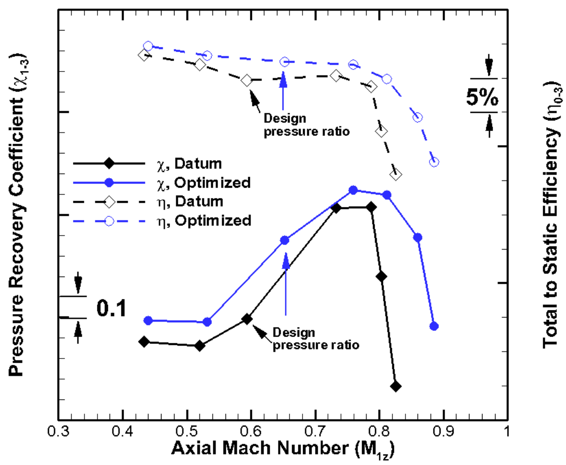

Fig. 15 Performance curve for the datum and the optimized turbine over a range of operating conditions

CONCLUSIONS

In the first part of this paper, challenges in designing a Low Pressure (LP) diffuser for steam turbine retrofits are demonstrated. Moreover, Alstom's in-house numerical method, which couples the last stage and the exhaust hood, Exhaust Design System (EDS), is validated against experimental measurements. The predicted performance agreed well with the measurements.

In the latter part of this paper, a re-designed diffuser casing is described for the retrofit of an LP steam turbine using the EDS method. To begin with, the axi-symmetric diffuser casing on the meridional plane was re-designed by carefully controlling the kink positions. Flows within the re-designed diffuser are well attached to the casing, resulting in a good pressure recovery, whereas the original diffuser shape caused substantial flow separations.

The axi-symmetrically re-designed diffuser casing was then further optimized, by introducing a circumferential variation of the diffuser casing, in order to take into account the full exhaust geometry. It was found out that the re-designed diffuser casing caused a blockage in the upper hood due to the increased diameter of the diffuser casing. In order to overcome this unfavorable feature, a cut-back in the upper hood was introduced, resulting in a circumferential asymmetry of the diffuser casing. This optimized diffuser casing improved the three-dimensional flow structure and maximized the performance of the LP diffuser and the exhaust hood.

This study highlights the importance of considering the full three-dimensional exhaust hood in designing the LP diffuser. Moreover, it is essential to take into account the interaction between the last stage and the exhaust hood without compromising the computational time.

REFERENCES

[1] Haller, B. R. and Hesketh, J. A., 1993, Large Steam Turbine Retrofitting to Improve Performance, Power-Gen Europe '93 Conference.

[2] Tindell, R. H., Alston, T. M., Sarro, C. A., Stegmann, G. C., Gray, L., and Davids, J., 1996, Computational Fluid Dynamic Analysis of a Steam Power Plant Low Pressure Turbine Downward Exhaust Hood, ASME J. Eng. For Gas Turbine and power, Vol. 118, pp. 212-224.

[3] Denton, J.. 1993, Loss Mechanisms in Turbomachines, J. of Turb. Vol. 115 , pp. 621-656.

[4] Sovran, G. and Klomp, E. D., Experimentally Determined Optimum Geometries for Rectilinear Diffusers with Rectangular, Conical or Annular Cross-section, Fluid Mechanics of Internal Flow, Elsevier Publishing Company, pp. 270-319, 1967.

[5] Liu, J. J., Yongqiang, C. and Hongde J., 2001, Investigation of Flow in a Steam Turbine Exhaust Hood with/without Turbine Exit Conditions Simulated, GT-2001-GT-0488.

[6] Kreitmeier, F. and Greim, R., 2003, Optimisation of Blade-Diffuser Interaction for Improved Turbine Performance, Proc. ImechE Part A, J. of Power and Energy, 217(4), pp 443-451.

[7] Fu, J. L. and Liu, J. J., 2010, Investigations of Influential Factors on the Aerodynamic Performance of a Steam Turbine Exhaust System, GT2010-22316.

[8] Cofer, J. I. IV, 1996, Advances in Steam Path Technology, J. Eng. Gas Turbine Power, ASME J. Eng. Gas Turbines for Power, Vol. 117, pp. 337-352.

[9] Craig and Cox, 1971, Performance Estimation of Axial Flow Turbine, I.Mech.E. Vol. 185, 32/71.

[10] Spencer, R. C., Cotton, K. C. and Cannon, C.N, 1974, A Method for Predicting the Performance of Steam Turbine-Generator… 16,500 KW and Larger, ASME Power Division, Paper No. 62-WA-209.

[11] Cotton K. C., 1998, Evaluating and Improving Steam Turbine Performance, 2nd Ed., Cotton Fact, USA.

[12] McBean, I,, Havakechian, S. and Masserey, P., The Development of long last stage steam Turbine Blades, GT2010-22747.

[13] Hongtao, W., Zhu, X. Zhaohui, D., and Yang, H., 2010, Aerodynamic Optimization System Development for Low Pressure Exhaust Hood of Steam Turbine, GT2010-22280.

[14] Liu, J. J. and Hynes, T. P., 2002, The Investigation of Turbine and Exhaust Interactions in Asymmetric Flows: Part 1 – Blade-Row Models Applied, GT-2002-30342

[15] Liu, J. J. and Hynes, T. P., 2002, The Investigation of Turbine and Exhaust Interactions in Asymmetric Flows: Part 2 – Turbine-Diffuser-Collector Interactions, GT-2002-30343

[16] Beevers, A., Conju, F., Pengue, F., and Mokulys, T., 2010, An analysis of the merits of CFD for the performance prediction of a low pressure steam turbine radial diffuser, GT2010-22107.

[17] Benim, A.C., Geiger, M., Doehler, S., Schoenenberger, M., and Roemer, H., 1995, Modelling the Flow in the Exhaust Hood of Steam Turbines Under Consideration of Turbine-Exhaust Hood Interaction, VDI Berichte NR 1185, pp. 343-357.

